**Proceedings of the ASME 2010 3rd Joint US-European Fluids Engineering Summer Meeting and 8th International Conference on Nanochannels, Microchannels, and Minichannels**
**FEDSM-ICNMM2010**
**August 1-5, 2010, Montreal, Canada**

# FEDSM-ICNMM2010-31137

# FLUID-STRUCTURE INTERACTION SIMULATION BY SMOOTHED PARTICLE HYDRODYNAMICS

**Mostafa Safdari Shadloo**
Sabancı University, Faculty of Engineering and Natural Sciences, PhD Student
İstanbul, Turkey

**Amir Zainali**
Sabancı University, Faculty of Engineering and Natural Sciences, MSc Student
İstanbul, Turkey

**Mehmet Yildiz**
Sabancı University, Faculty of Engineering and Natural Sciences, Faculty Member
İstanbul, Turkey

## ABSTRACT

In this article, a modified SPH algorithm is proposed to solve Fluid-Structure Interaction (FSI) problems including fluid flow in interaction with compatible structures under a large deformation. To validate the current algorithm against available data in literature, we consider two important benchmark cases; namely, an oscillating elastic beam and dam breaking problems. The proposed algorithm is based on the elimination of the intermediate data transfer steps between the fluid and the solid structures, whereby resulting in an easy and time-saving simulation method. With the test application studied, we were able to prove the ability of the modified SPH method for solving of fluid and solid domains monolithically without the need to define an interfacial boundary condition or any additional steps to simulate the deformation of an elastic dam. Numerical results suggest that upon choosing correct SPH parameters such as smoothing function, and lengths, as well as coefficients for artificial viscosity and artificial stress, one can obtain results in satisfactorily agreement with numerical findings of earlier works.

## INTRODUCTION

Fluid-Structure interaction (FSI) is one of the challenging problems in the field of computational fluid dynamics. Typical examples include flow around aircrafts, wings and bridges, fluid flow inside blood vessels, the FSI inside safety valves for pressure reduction and many other complex structures. In general, Lagrangian-Eulerian methods (LE) have been used in literature, which implement Eulerian formulation for fluid and Lagrangian formulation for solid structures. However these approaches, when the deformation of the solid structure is large, face numerous difficulties such as transferring data between fluid and the solid structure [1,2]. To overcome these modeling difficulties, it would be a prudent choice to use Lagrangian formulations for both fluid and solid sites, because Lagrangian methods can solve the governing equations of fluid and structure simultaneously without implementing any specific treatment for data transfer from one region to another.

Smoothed particle hydrodynamics (SPH) is one of the members of meshless Lagrangian particle methods used to solve partial differential equations widely encountered in scientific and engineering problems [3]. The Lagrangian nature of this method makes it a viable and powerful tool to simulate a variety of complex fluid flow processes such as FSI. In this work a modified SPH algorithm is proposed to solve problems including fluid flow in interaction with compatible structures under a large deformation. The modification of this algorithm is based on eliminating the intermediate data transfer steps terms, which results in an easy and time-saving numerical simulation method.

The current presentation is structured as follows; in section 2, having introduced governing equations for both fluid and solid constituents along with the relevant constitutive relations, we provide a brief description of the solution algorithm. In section 3, first two test cases, namely, oscillating plate and dam breaking problems are validated against available numerical data. These two test cases are combined into a third test application, whereby forming a dam breaking problem with an elastic gate, for which results are also presented. The

presentation is concluded in section 4 with a brief discussion and remarks on the results presented herein.

**Keywords:** Smoothed Particles Hydrodynamic (SPH), Fluid-Structure Interaction (FSI), Elastic plate, Dam breaking problem

## NOMENCLATURE

| | |
|---|---|
| $\vec{\mathbf{a}}_\mathbf{i}$ | Acceleration vector |
| $C_o$ | Speed of the sound |
| D | Length of dam breaking container |
| d | Height of dam breaking container |
| $\underline{\underline{\mathbf{d}}}$ | Deformation rate tensor |
| $f(x)$ | Natural frequency of the plate |
| $\vec{\mathbf{f}}_{\mathbf{ij}}$ | Force on a particle **i** exerted by particle **j** |
| $\vec{\mathbf{g}}$ | Gravitational acceleration |
| H | Characteristic height |
| $h$ | Smoothing length |
| K | Bulk modules |
| $kL$ | Fundamental mode |
| L | Characteristic length |
| $l_o$ | Initial particle spacing |
| $m_\mathbf{i}$ | Mass of particle **i** |
| $p$ | Pressure |
| $\vec{\mathbf{r}}_\mathbf{i}$ | Position vector |
| $r_{\mathbf{ij}}$ | Magnitude of distance between particle **i** and **j** |
| $\underline{\underline{\mathbf{R}}}_{\mathbf{ij}}$ | Artificial stress tensor |
| $\underline{\underline{\mathbf{S}}}$ | Deviatoric stress tensor |
| $t$ | Time |
| $\vec{\mathbf{v}}$ | Velocity vector |
| $W$ | Kernel function |
| $\alpha$ | Artificial viscosity coefficient |
| $\alpha_o$ | Spline coefficient |
| $\beta$ | Kernel ratio |
| $\delta_{kl}$ | Kronecker delta |
| $\mu$ | Shear modules |
| $\underline{\underline{\boldsymbol{\tau}}}$ | Shear stress tensor |
| $\psi_\mathbf{i}$ | Number density of particle **i** |
| $\underline{\underline{\boldsymbol{\omega}}}$ | Vorticity tensor |
| $\Pi_{\mathbf{ij}}$ | Artificial viscosity |
| $\rho$ | Density |

## THEORY OF THE MODEL

*Governing equations:*

The governing equations used to solve both the fluid and solid problems in this article are the mass and linear momentum balance equations which are expressed in the Lagrangian form and given in direct notation, respectively as

$$d\rho/dt = -\rho\nabla\bullet\vec{\mathbf{v}} \tag{1}$$

$$\rho d\vec{\mathbf{v}}/dt = -\nabla p + \nabla\bullet\underline{\underline{\boldsymbol{\tau}}} + \rho\vec{\mathbf{g}} \tag{2}$$

Given that inertial forces are dominant over viscous ones for the problems considered herein, the fluid is treated as inviscid; as a result, one can neglect the viscous forces in the computations, $\underline{\underline{\boldsymbol{\tau}}} = 0$. Assuming that the relation $S_{kl} = \tau_{kl}$ holds for an elastic plate, on using Hook's law corrected by Jaumann's rate, the deviatoric stress tensor for hypoelastic materials can be defined as [4],

$$\frac{DS_{kl}}{Dt} = 2\mu(d_{kl} - \frac{1}{3}\delta_{kl}d_{mm}) + S_{km}\omega_{lm} + \omega_{km}S_{ml} \tag{3}$$

while the deformation rate and vorticity (spin) tensors are defined, respectively as

$$d_{kl} = 0.5(v_{k,l} + v_{l,k}) \tag{4}$$

$$\omega_{kl} = 0.5(v_{k,l} - v_{l,k}) \tag{5}$$

where $\mu$ is the shear modulus. Equation (3) allows consideration of path dependence and non-linearity in stress-strain response.

*SPH formulation:*

The integral estimate or the kernel approximation to an arbitrary function $f(\vec{\mathbf{r}}_\mathbf{i})$ can be introduced as

$$f(\vec{\mathbf{r}}_\mathbf{i}) \cong \langle f(\vec{\mathbf{r}}_\mathbf{i})\rangle \equiv \int_\Omega f(\vec{\mathbf{r}}_\mathbf{j})W(r_{\mathbf{ij}},h)d^3\vec{\mathbf{r}}_\mathbf{j} \tag{6}$$

where $W(r_{\mathbf{ij}},h)$ is a smoothing or kernel function and the length $h$ defines the support domain of the particle of interest. Replacing the integration in Equation (6) with SPH summation over particle "**j**" and setting $d^3\vec{\mathbf{r}}_\mathbf{j} = 1/\psi_\mathbf{j}$, we can write SPH interpolation for an arbitrarily field $A_\mathbf{i}$ as.

$$A_{\mathbf{i}} = A(\vec{\mathbf{r}}_{\mathbf{i}}) = \sum_{\mathbf{j}}^{N} \frac{1}{\psi_{\mathbf{j}}} A_{\mathbf{j}} W\left(r_{\mathbf{ij}}, h\right) \tag{7}$$

where the number density $\psi_{\mathbf{i}}$ for the particle **i** is defined as

$$\psi_{\mathbf{i}} = \sum_{\mathbf{j}}^{N} W\left(r_{\mathbf{ij}}, h\right) \tag{8}$$

which is equal to reciprocal of the corresponding particle's volume.

The SPH approximation for the gradient of the arbitrary function $A_{\mathbf{i}}$ can be introduced as

$$\nabla A_{\mathbf{i}} = \sum_{\mathbf{j}=1}^{N} \frac{1}{\psi_{\mathbf{j}}} \left(A_{\mathbf{j}} - A_{\mathbf{i}}\right) \nabla W\left(r_{\mathbf{ij}}, h\right) \tag{9}$$

Throughout the present simulations, the compactly supported two-dimensional cubic and quintic splines, with a smoothing radius, $\kappa h$, are used, which are given in Eqs. (10) and (11) as

$$W\left(r_{\mathbf{ij}}, h\right) = \alpha_o \begin{cases} 2/3 - s_{\mathbf{ij}}^2 + s_{\mathbf{ij}}^3/2 & \textbf{if } 0 \le s_{\mathbf{ij}} < 1 \\ \left(2 - s_{\mathbf{ij}}\right)^3/6 & \textbf{if } 1 \le s_{\mathbf{ij}} < 2 \\ 0 & \textbf{if } s_{\mathbf{ij}} \ge 2 \end{cases} \tag{10}$$

$$W\left(r_{\mathbf{ij}}, h\right) = \alpha_o \begin{cases} \left(3 - s_{\mathbf{ij}}\right)^5 - 6\left(2 - s_{\mathbf{ij}}\right)^5 + 15\left(1 - s_{\mathbf{ij}}\right)^5 & \textbf{if } 0 \le s_{\mathbf{ij}} < 1 \\ \left(3 - s_{\mathbf{ij}}\right)^5 - 6\left(2 - s_{\mathbf{ij}}\right)^5 & \textbf{if } 1 \le s_{\mathbf{ij}} < 2 \\ \left(3 - s_{\mathbf{ij}}\right)^5 & \textbf{if } 2 \le s_{\mathbf{ij}} \le 3 \\ 0 & \textbf{if } s_{\mathbf{ij}} \ge 3 \end{cases} \tag{11}$$

Here, $s_{\mathbf{ij}} = r_{\mathbf{ij}}/h$ and spline coefficient $\alpha_o$ is equal to $15/7\pi h^2$ and $7/478\pi h^2$ for cubic and quintic splines, respectively and $\kappa$ is a coefficient that is equal to 2 and 3 for cubic and quintic splines, respectively.

The particle density can be discretized based on the calculated values of mass and number density at each point in the following way,

$$\rho_{\mathbf{i}} = m_{\mathbf{i}} \psi_{\mathbf{i}} \tag{12}$$

The acceleration of a particle can be calculated using the relation

$$\vec{\mathbf{a}}_{\mathbf{i}} = \frac{1}{m_{\mathbf{i}}} \sum_{\mathbf{j}}^{N} \vec{\mathbf{f}}_{\mathbf{ij}} \tag{13}$$

where the force on a particle, $\vec{\mathbf{f}}_{\mathbf{ij}}$ is given by,

$$\vec{\mathbf{f}}_{\mathbf{ij}} = -\left[\left(\frac{p_{\mathbf{i}}}{\psi_{\mathbf{i}}^2} + \frac{p_{\mathbf{j}}}{\psi_{\mathbf{j}}^2} - \alpha \prod_{\mathbf{ij}}\right) \underline{\underline{\mathbf{I}}} - \underline{\underline{\mathbf{R}}}_{\mathbf{ij}} \beta^q\right] \bullet \nabla W\left(r_{\mathbf{ij}}, h\right) + m_{\mathbf{i}} \vec{\mathbf{g}} \tag{14}$$

where $\beta = W\left(r_{\mathbf{ij}}, h\right)/W\left(l_o, h\right)$ is the kernel ratio, and $l_o$ is the initial particle spacing between two neighbours, and $q$ is an exponential factor which is selected to be 4. Here, $\prod_{\mathbf{ij}}$ is the artificial viscosity which acts on all of the particles and has a stabilizing role on the numerical solution [3] while $\underline{\underline{\mathbf{R}}}_{\mathbf{ij}}$ is the so-called artificial stress which acts only on the elastic solid particles [5].

The second order Verlet's time stepping scheme is implemented for time integration. In this scheme, the particle velocity, density, and positions are updated according to,

$$\vec{\mathbf{r}}_{\mathbf{i}}^{\,n+1/2} = \vec{\mathbf{r}}_{\mathbf{i}}^{\,n} + 0.5\Delta t \vec{\mathbf{v}}_{\mathbf{i}}^{\,n} \tag{15}$$

knowing the intermediate particle positions, it should be noted one can determine the intermediate density either using equation (1) (discretized with equation (9)) or directly from equation (12). In this work, the latter approach is used. Then pressure is calculated by,

$$p - p_o = c^2\left(\rho - \rho_o\right) \tag{16}$$

where *c* is assumed to be a speed of the sound which should be big enough to enforce the incompressibility condition [6-8]. At the end, final particle positions and velocities are calculated by,

$$\vec{\mathbf{v}}_{\mathbf{i}}^{\,n+1} = \vec{\mathbf{v}}_{\mathbf{i}}^{\,n} + \Delta t \vec{\mathbf{a}}_{\mathbf{i}}^{\,n} \tag{17}$$

$$\vec{\mathbf{r}}_{\mathbf{i}}^{\,n+1} = \vec{\mathbf{r}}_{\mathbf{i}}^{\,n+1/2} + 0.5\Delta t \vec{\mathbf{v}}_{\mathbf{i}}^{\,n+1} \tag{18}$$

### *The treatment of the fluid and solid interface*

There are two types of particles inside the whole computational domain. The first type consists of particles whose distance from the interface is greater than the smoothing length. These particles are allowed to interact only with particles of the same species (particle $a_1$ as shown in figure 1), whereas the second type of particles have influence domain truncated by the other region so that their influence domains are populated by both types of particles. Therefore, the second type can interact with particles of both sides (particle $a_2$ as also shown in figure 1). Here, the term species refers to solid and liquid particles.

Antoci et al. [9] solved the equations of motion for each species separately. In their approach, the force exerted by fluid particles on a given solid particle with the kernel truncation by the interface is calculated, which is an action force. To ensure that Newton's third law, which states that the forces of action and reaction between two bodies are equal, is not violated, they associated near interface fluid particles with the same magnitude of the calculated force but with the negative sign, which corresponds to the computation of reaction force. This approach requires the computation of interface normal to interpolate forces from solid particles on the fluid particles, as well summations for force integration, thereby being a computationally difficult and expensive methodology.

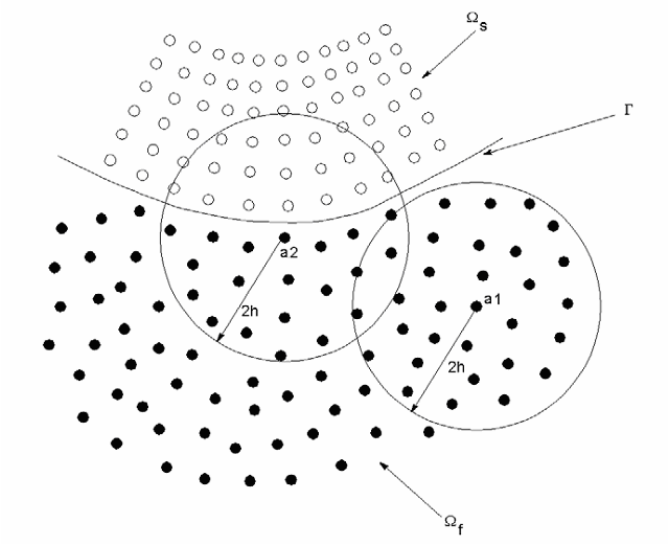


Figure 1. Sketch of the domain near the interface where particle a1 and a2 represent particles of type 1 and 2, respectively.

Towards this end, we proposed here a new approach which solves the one set of equations for the whole domain which is rather simpler and computationally faster due to the elimination of the intermediate steps for calculating the interface normal and also transferring the force from one species to another. In our approach, we solve only one set of equations for the particles of the whole domain, noting that for calculating the pressure term, $\left(p_i/\psi_i^2 + p_j/\psi_j^2\right)$, we have to account for the pressure of the all neighboring particles without considering their species. It is fruitful to mention that, since the pressure term is symmetric it naturally satisfy the action-reaction principle.

## RESULTS AND DISCUSSION

In this section, numerical results for two test cases, elastic beam and dam breaking, are presented. The results are validated against available numerical data in literature.

*Elastic beam:*

The geometry of elastic beam modeled is shown in figure 2. The initial velocity, considering the analytical free oscillations of a thin plate, is given by,

$$v_y(x) = v_{L0} C_0 f(x) / f(L) \tag{19}$$

where the natural frequency $f(x)$, and speed of sound inside the solid $C_0$ are defined as,

$$f(x) = \left(\cos(kL) + \cosh(kL)\right) * \left(\cosh(kx) - \cos(kx)\right) + \left(\sin(kL) - \sinh(kL)\right) * \left(\sinh(kx) - \sin(kx)\right) \tag{20}$$

$$C_o = \left(K/\rho_o\right)^{0.5} \tag{21}$$

while the initial velocity of the free end is assumed to be equal to $v_{L0} = 0.01$ *m/s*. Also the fundamental mode, *kL* is set to be 1.875 in this study. The results are shown for simulation parameters of $\rho$=1000 *kg/m*$^3$, L=0.2 *m*, H=0.02 *m*, K=3.25×10$^6$ (N/m$^2$) and $\mu$=715000 (N/m$^2$), where K and μ are the bulk and shear modules of the solid, respectively.

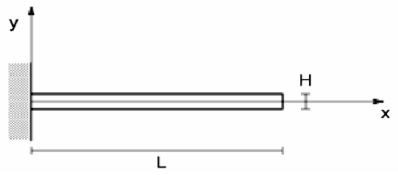


Figure 2. Sketch of the plate.

In figure 3, the profiles of the ratio of the fifth to the first amplitude of the free surface oscillation are shown for the different smoothing lengths as a function of artificial viscosity coefficient and compared to the results presented in [9]. It can be seen that the results are in excellent agreement with those of literature [9]. The figure shows the effects of the artificial viscosity on variations of the amplitude ratio ($A_5$ /$A_1$) and also the effects of ratio of the smoothing length to the initial particle spacing. It is observed that the results are unstable for $\alpha$=0. One can also conclude from figure 3 that with increasing artificial viscosity, damping of the free oscillation is reduced. This can be due to the particle disorder induced by plate oscillation, while increasing the artificial viscosity remedies this problem.

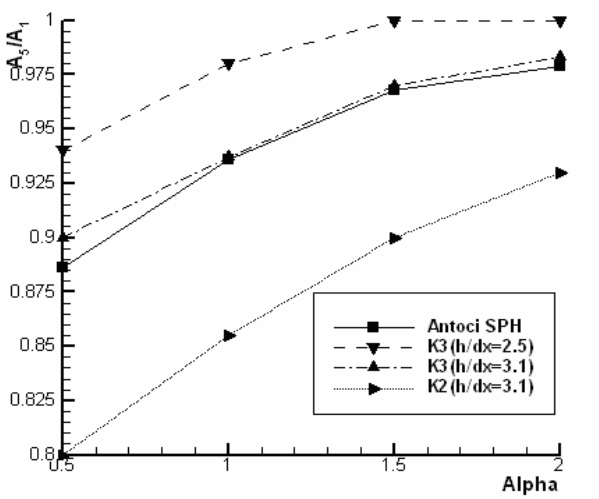


**Figure 3.** The ratio of the fifth to first amplitude of the free surface oscillation are shown for the different smoothing lengths as a function of artificial viscosity. Here, K3 in the above the legend indicates the results obtained with a quintic spline, while K2 is with a cubic spline.

*Dam breaking:*

The initial geometry of dam breaking considered is shown in figure 4. the space occupied by the fluid at time=0 is indicated by x in figure 4. In this test case, the following input parameters are used; L/H=3, D/H=3, d/H=5.336, $p_0/\rho gh$=17.4 .

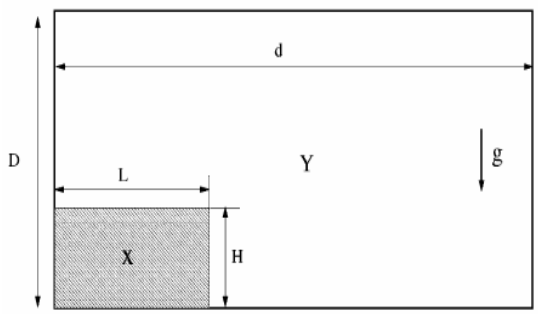


Figure 4. The sketch of the dam breaking.

To be able to implement boundary conditions for the free surface, the free surface particles should be identified to distinguish them from interior fluid particles. Since the kernel function of particles that are on or in the close vicinity of the free surface is truncated; the particle number density $\psi_i$ for these particles will drop. Particles with the number densities below a preset threshold value are recognized as free surface particles: namely, $\psi_i \le 0.9\psi_{i,ref}$ ,where $\psi_{i,ref} = \max(\psi_i)$ . All free surface particles are assigned to zero pressure. Additionally, in the calculation of the artificial viscosity, to enforce free slip (also referred to as symmetry) boundary condition on solid walls, ghost particles are created by means of mirroring fluid particles with respect to solid walls and then assigned with the velocities such that $v_t = v_{gt}, v_n = -v_{gn}$ (where ghost particle is denoted by subscript g).

Figure 5 illustrates the evolution of liquid front toe. The comparison of numerical results obtained here shows a good agreement with those presented in [10].

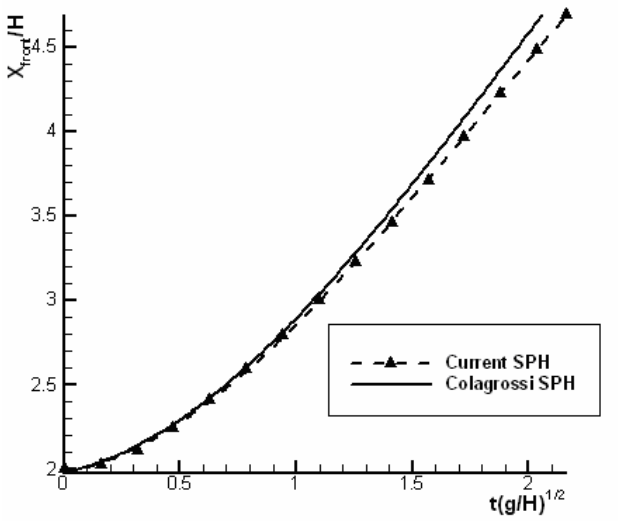


Figure 5. Liquid front toe as a function of time.

*Dam breaking problem with an elastic gate*

The two previously presented test cases are combined into a third test application, whereby forming a third benchmark problem which is the deformation of elastic gate subjected to the dam breaking. The geometrical configuration of the problem is shown in figure 6. The upper wall is rigid while the lower wall (elastic gate) can deform.

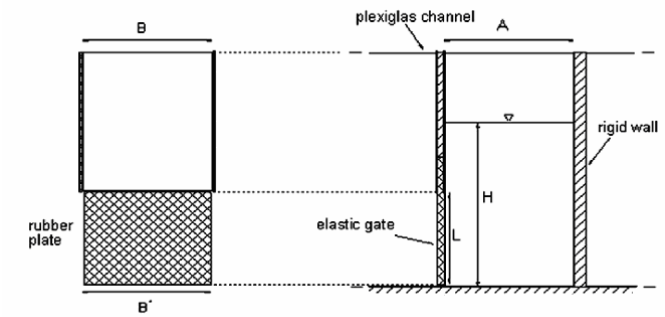


**Figure 6.** A sketch of the dam breaking problem with an elastic gate front view (left), side view (right).

The input parameters for the model are: $\rho$=1100(kg/m$^3$), E=10(MPa), A=0.1(m), B=0.1(m), B$^*$=0.098(m), H=0.14, L=0.079, S=0.005. On solid boundaries, free slip boundary

condition imposed as before. This problem is solved using the modified SPH algorithm explained previously for the times between 0-4 s. The results for time intervals of 0, 1, 2 and 4 s. are shown in figure 7.

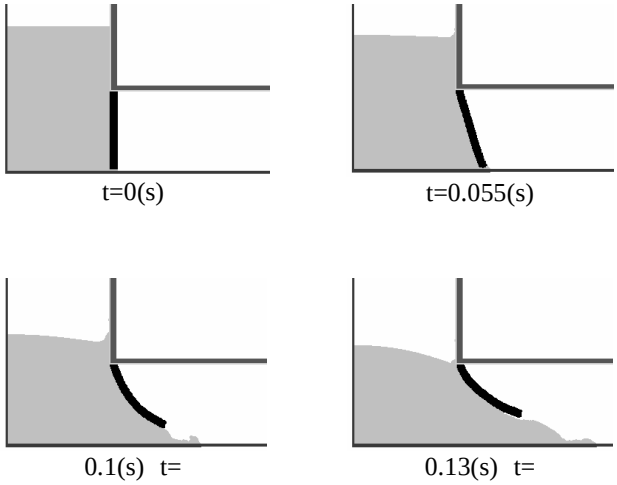


**Figure 7.** Position of the elastic gate for different time steps (side view).

## CONCLUSION

The modified algorithm was validated by simulating an oscillating elastic beam and a dam breaking problem with free surface. These two test cases were combined into a test application problem for which we solved a dam breaking problem with an elastic gate. The fluid is treated as inviscid, while the elastic gate is modeled through an incremental hypoelastic relation. With the test application, we showed the ability of the modified SPH method for solving of fluid and solid domains monolithically without the need to define an interfacial boundary condition or any additional step to simulate the deformation of an elastic dam. Numerical results suggest that upon choosing correct SPH parameters such as smoothing function, and lengths, as well as coefficients for artificial viscosity and artificial stress, one can obtain results in agreement with experimental findings.

## ACKNOWLEDGEMENTS:

Funding provided by the European Commission Research Directorate General under Marie Curie International Reintegration Grant program with the Grant Agreement number of 231048 (PIRG03-GA-2008-231048) is gratefully acknowledged.

## REFERENCES

[1] Rugonyi S, Bathe KJ. On finite element analysis of fluid flows fully coupled with structural interactions. Comput Model Eng Sci., 2:195–212, 2001.
[2] Bathe KJ, Zhang H. Finite element developments for general fluid flows with structural interactions. Int J Numer Methods Eng., 60:213–32, 2004.
[3] Monaghan J.J., Smoothed particle hydrodynamics, Reports on Progress in Physics, 68, 1703–59, 2005.
[4] Lai W.M., Rubin D., Krempl E., Introduction to Continuum Mechanics, USA, Butterworth Heinemann Ltd., 3rd ed., 1996.
[5] Gray J.P, Monaghan J.J., Swift R.P., SPH elastic dynamics. Comput. Methods Appl. Mech.Eng.190,6641–62, 2001.
[6] Morris J.P., Fox P.J., Zhu Y., Modeling low Reynolds number incompressible flows using SPH, Journal of Computational Physics, 136:1, 214-26, 1997.
[7] Monaghan J.J., Cas R.A.F., Kos A.M., Hallworth M. Gravity currents descending a ramp in a stratified tank. J Fluid Mech., 379, 39–69, 1999.
[8] Gallati M., Braschi G., Simulazione Lagrangiana di flussi con superficie libera in problemi di idraulica, L'acqua, 5, 7–18, 2000.
[9] Antoci C., Gallati M., Sibilla S., Numerical simulation of fluid–structure interaction by SPH, Journal of Computers and Structures, 85, 879-890, 2007.
[10] Colagrossi A., Landrini M., Numerical simulation of interfacial flows by smoothed particle hydrodynamics, Journal of Computational Physics, 191, 448–475, 2003.